Newcastle University

ePrints

Washington JG, Atkinson GJ, Baker NJ. Reduction of Cogging Torque and EMF Harmonics in Modulated Pole Machines. *IEEE Transactions on Energy Conversion* 2016, DOI: 10.1109/TEC.2016.2520200

Copyright:

© 2016 IEEE. Personal use of this material is permitted. Permission from IEEE must be obtained for all other uses, in any current or future media, including reprinting/republishing this material for advertising or promotional purposes, creating new collective works, for resale or redistribution to servers or lists, or reuse of any copyrighted component of this work in other works.

DOI link to article:

http://dx.doi.org/10.1109/TEC.2016.2520200

Date deposited:

14/03/2016

Newcastle University ePrints - eprint.ncl.ac.uk

Reduction of Cogging Torque and EMF Harmonics in Modulated Pole Machines

J. G. Washington, G. J. Atkinson, N. J. Baker

Abstract – This paper discusses a method for reducing cogging torque and harmonic content of back EMF waveforms in modulated pole machines (MPMs). Tooth pitching is applied to a separate phase MPM in order to reduce the most prominent harmonics present in a three-phase MPM's cogging torque. Experimental results show that the application of tooth pitching to these machines can reduce the cogging torque and back EMF harmonics significantly. This comes without a significant impact to the useful output of the machine, which is confirmed by comparison of measured results for two prototypes. Such a technique can be easily applied to existing machine designs without the need for extra components and for the same production cost.

Index Terms—Permanent magnet, three-phase, transverse flux, AC Machine. cogging torque, harmonics, pitching.

I. Introduction

MODULATED Pole Machines (MPMs) such as Transverse Flux [1-5] and Claw Pole [6-8] machines are known for their ability to produce a high torque relative to their volume. This has made them desirable for direct drive applications where a high torque is required at a low rotational speed, such as traction applications [9-10], wind turbines [11], and wave energy converters [12].

MPMs differ from conventional longitudinal flux machines in the fact that the electrical and magnetic circuits of the machine are effectively decoupled. The performance of the magnetic circuit is determined by the teeth and core-back of the machine. The number, size, and circumferential position of the teeth can be set independently of the size of the coil, which determines the electrical performance of the machine for a given thermal limit.

Furthermore, as the magneto-motive force (MMF) of the coil is seen across all the teeth of the machine, an increase in the tooth number (effectively a reduction in the pole pitch) leads to an increase in the electrical loading of the machine [13]. This property means that MPMs tend to have a high pole number, 50-100 poles is not unusual.

MPMs suffer from a common set of drawbacks, namely a high cogging torque (and consequently a high torque ripple) [2], and a low power-factor [14]. The aim of this paper is to explore and analyse a technique to reduce the cogging torque of the machine.

Typical techniques for reducing cogging torque in MPMs (and synchronous machines in general) have included; current shaping [15], tooth shape optimisation [16, 17], rotor or stator skew [17-19], and shifting of the stator components in a phase so they are not 180° apart [20-22], amongst others. A technique whereby the teeth of the machine are pitched in order to reduce the cogging torque of the machine will be investigated. It will be shown that the same technique also reduces harmonic content of the back EMF waveform, which when combined with the cogging torque is important in determining the torque ripple of the machine.

The term "Modulated Pole Machine" is used here to capture all machine types where the field generated by a coil is guided or "modulated" into many poles by the surrounding toothed iron stator structure, this is a property common to Claw Pole and Transverse Flux Machines. This paper is concerned with a Modulated Pole Machine of the Transverse Flux type, although the techniques discussed are applicable to any MPM.

II. Single Phase Machines

Cogging torque is an effect common to all slotted permanent magnet machines. It stems from the tendency of the permanent magnets and pole pieces in the rotor to line up with the stator teeth in such a way as to minimise the reluctance of the magnetic circuit when no current is applied. In conventional machines a low cogging torque can be achieved by an appropriate choice of a slot/pole combination with a high common multiple [23, 24]. This is not the case in MPMs.

The basic operation of an MPM requires that there are an equal number of teeth and poles, therefore at a number of points in an electrical cycle all teeth align with a pole in the position of minimum reluctance. When the poles and teeth are aligned a single phase machine cannot reliably start. The equal number of teeth and poles also leads to a high cogging torque with a low frequency in comparison to the electrical frequency.

Fig. 1 shows a single pole-pair of a single-phase outer rotor MPM. The rotor is constructed from soft magnetic composite (SMC) poles and circumferentially magnetised permanent magnets, these alternate in their direction of magnetisation around the circumference of the machine, in the standard flux concentrating style.

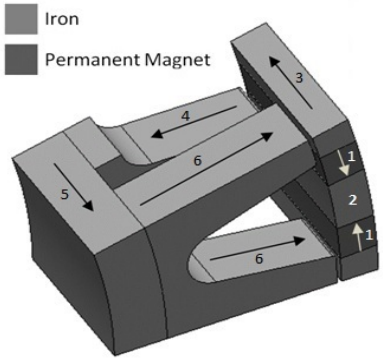

Fig. 1. A two pole section of a single-phase MPM showing its flux paths, the coil is not shown for clarity.

Jamie Washington is with the Electric Drive System Group, Höganäs AB, Höganäs, SE-263-83 Sweden (e-mail: Jamie.Washington@Hoganas.com).

Glynn Atkinson and Nick Baker are with the Department of Electrical and Electronic Engineering, Newcastle University, Newcastle Upon Tyne, NE1 7RU, United Kingdom. (email: Glynn.Atkinson@ncl.ac.uk, Nick.Baker@ncl.ac.uk).

The rotor is aligned in the d-axis; the position of maximum flux linkage and minimum reluctance. The permanent magnets (1) deliver flux into the central rotor pole (2). The flux travels down this pole and across the air gap into the stator tooth (4), around the core-back (5), and splits between the two teeth of the opposite stator half (6), which is displaced circumferentially 180° electrical from tooth (4). Finally the flux crosses the air gap, once again returning to the magnets through the outer poles (3).

During an electrical cycle the rotor passes through up to eight detent (zero) torque positions. Four of these are always present, two due to magnet fringing (q-axis), two due to the magnetised rotor poles (d-axis). Up to four more can exist due to the interaction of these effects, which is the case during this analysis.

Considering the permanent magnets first, as they move toward the centre of the tooth tip (q-axis position) there is a stable position where the magnets are shorted via the rotor pole edge, air-gap and tooth tip, as shown in the left pane of Fig. 2. In this position the rotor pole edges are heavily saturated by the shorted flux and tend toward the permeability of free space. In effect the magnet fringing flux is acting alone without being influenced by the pole pieces.

Displacing the rotor either side of the q-axis creates a positive or negative torque, as shown in Fig. 3. Once the magnets move toward the outer edge of the tooth tip they are no longer shorted and the magnet flux redirects through the now unsaturated rotor pole pieces. Magnet fringing no longer acts as the cogging torque source and the magnetised rotor pole pieces become the dominant flux path.

Now considering the rotor pole pieces; when centred over the stator tooth tip (d-axis position), as shown in the right hand pane of Fig. 2, there is magnetic alignment and zero torque. Rotation away from this position generates a torque to return the rotor to the d-axis. Torque increases until the magnets begin to short once again and the flux is directed away from the pole piece.

The two contributions to cogging torque are therefore associated with magnet fringing and the magnetised pole piece.

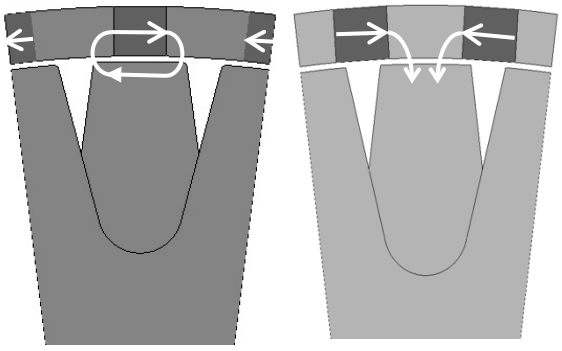

Fig. 2. Two pole section of a single phase MPM with rotor positioned in the q-axis (left) and the d-axis (right).

The magnet fringing torque is only present when the magnet is interacting directly with the stator tooth, beyond this point the magnet flux is redirected into the pole piece and the magnetised pole piece torque contribution becomes dominant. The pole pieces only create torque when they interact with the stator tooth. Both torque waveforms can be described by Equation 1;

$$T_{cog} = -M\sin\left(\frac{2\pi\theta}{\lambda}\right) \ between \ \pm\frac{\lambda}{2} \ and \ 0 \ elsewhere \quad (1)$$

Where M is the peak torque contribution of the magnet fringing or magnetised pole pieces, θ is the rotor position and λ is the angular span of the magnet or rotor pole piece in question. For the machine being discussed here, the magnet span is 38° and pole piece span is 142°.

Summing the magnet fringing and magnetised pole piece torque contributions, with each placed onto their respective q and d axis, gives the analytical single phase cogging torque waveform shown in Fig. 3. In this analysis the fringing torque contribution has been set to 10% of the magnetised pole piece torque contribution, note the similarity with the FEA analysis of a MPM in Fig. 4 and that derived in the detailed analytical study by Masmoudi [29].

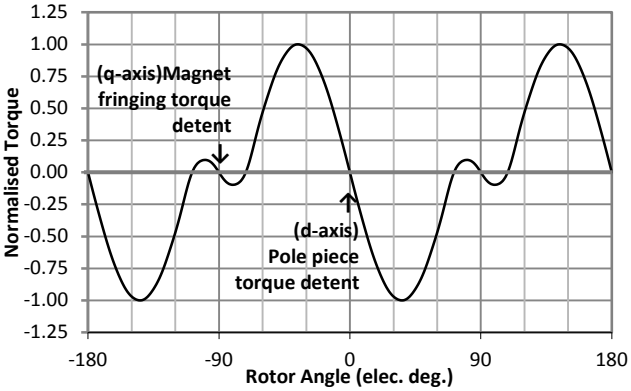

Fig. 3. Analytical cogging torque model based on the sum of magnet fringing and magnetised rotor pole piece torques.

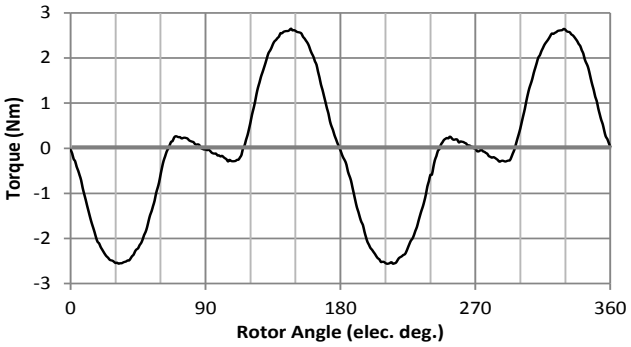

Fig. 4. The cogging torque of a single-phase MPM over one electrical cycle, obtained from a finite element model.

III. Three-Phase Machines

The cogging torque analytical model has been extended to include the Fourier analysis of the two torque components, the series for each given by the equation;

$$T_{cog} = \frac{\lambda}{\pi}\sum_{n=1}^{\infty}\sin(n\theta)\left(\frac{\sin\left(\pi+\frac{n\lambda}{2}\right)}{2\pi+n\lambda} - \frac{\sin\left(\pi-\frac{n\lambda}{2}\right)}{2\pi-n\lambda}\right) \quad (2)$$

Where *n* is the harmonic number under consideration. The harmonics for the fringing and pole piece components are calculated and then displaced appropriately to place the torque component on the q or d axis. The cogging torque waveform for a single phase, shown in Fig. 3, has been reconstructed from the harmonics generated by the analytical model.

Fig. 5 shows an axial view of a typical three-phase MPM arrangement, composed of three single-phase MPM units with an axial separation. This separation needs to be

significantly larger than the air gap and acts to reduce the amount of mutual coupling between adjacent phases, this machine will be termed a separate-phase machine.

Tooth 1 denotes the two teeth enclosing the coil A, this is phase A, tooth 1 and 1' are displaced 180° apart circumferentially. To create a balanced three-phase arrangement tooth 2 of phase B is displaced 120° from tooth 1, and tooth 3 of phase C a further 120°.

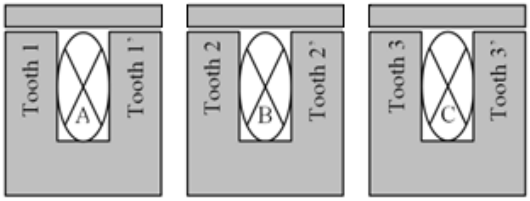

Fig. 5. Axial view of a three-phase MPM with axial separation.

The single phase harmonic components are therefore also displaced by 0º,120 º and 240 º and summed to form the set of three-phase cogging torque harmonics. This set of harmonics are reconstructed to give the total cogging torque waveform shown in Fig. 6, this waveform shape is very similar to that shown later in the measured results.

This analysis shows the complete cancellation of the magnetised pole piece component, with only the magnet fringing effect contributing to cogging torque. The harmonic spectrum of this analytical waveform, shown in Fig. 7 indicates a highly dominant 6th harmonic, the reduction of which forms the subject of the following sections.

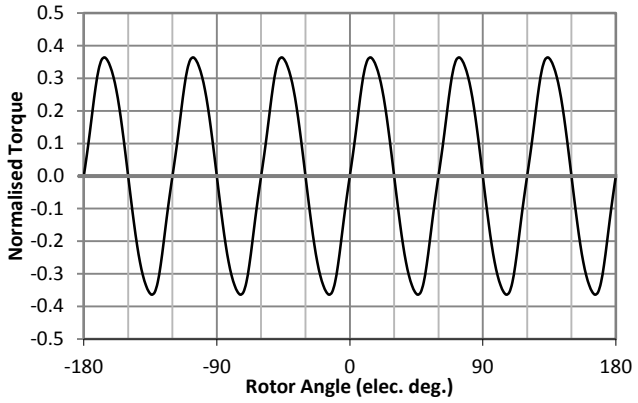

Fig. 6. Three phase cogging torque waveform reconstructed from the harmonics of the analytical cogging torque model. Magnet span = 38°, pole span = 142°.

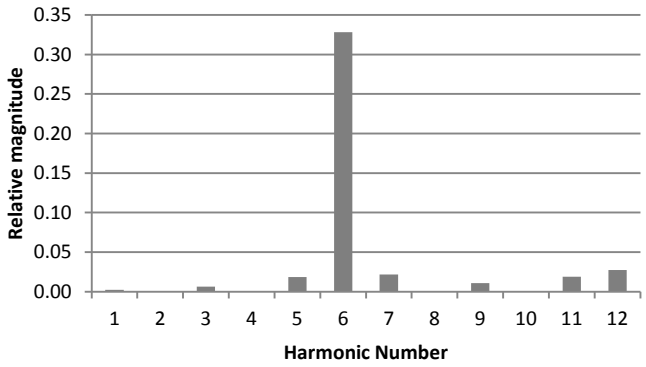

Fig. 7. Harmonic spectra of the analytical cogging torque waveform.

Although cogging torque is a large factor in the torque ripple of an MPM, the harmonic content in the back EMF waveform is also known to contribute, especially at high electrical loading. Machines of this type can exhibit high harmonic content especially on load, as was shown in [25]. In order to best produce a machine with a low ripple the reduction of both cogging torque and harmonic content will be considered.

IV. Tooth Pitching

Conventional machines use the concept of coil pitching to reduce harmonic content in the voltage waveforms in order to produce a smoother torque or current. This approach is not possible in MPMs due to the fact that the coils are simple hoops placed between two toothed stator components. It is these components that guide the two pole field of the coil into a multi-pole field, with a pole number equal to the number of teeth surrounding the coil. Conversely, it is these teeth that guide the air gap flux from the magnets around the coil, hence modifying these teeth can change the flux linking the coils of the machine.

It is therefore suggested that instead of pitching the coils, as in conventional radial flux machines, the teeth be shifted or 'pitched'. In conventional machines pitching the coil changes the flux that is linked, rather than the path of the magnet flux itself. In the MPM, changing the position of the teeth will change the flux path. This means that by moving the teeth, factors affected by the magnetic circuit of the machine, such as cogging torque, can be reduced in addition to the harmonics of induced voltage. This is exactly the same effect as moving the position of the teeth (rather than the coils) in a conventional machine as applied in [26]. The result is a set of fully pitched teeth with fluxes at their original position, and a set of pitched teeth with the fluxes shifted by the pitching angle, with the resultant flux the vector sum of the two sets of teeth.

A method of symmetrical shifts has been applied to an axial flux MPM, finite element calculations suggested a beneficial reduction in torque ripple [27].

Consider, for example a 'fully pitched' MPM, each tooth on a single stator component is placed a full electrical cycle circumferentially from the next. A second stator segment is placed next to this with the component rotated by 180° electrical relative to the first, this produces the situation shown in Fig. 1, and is the standard setup for an MPM.

This equal spacing of teeth is repeated in the left pane of Fig. 8 for clarity. To replicate coil pitching in a conventional machine, at regular intervals a tooth needs to be closer to, then further away from the neighbouring teeth. This is shown in the right pane of Fig. 8. In this case the tooth has been pitched by 60° electrical to exaggerate the effect, the middle tooth has been moved clockwise 60° and is now closer to the first tooth and hence 60° further away from the next tooth. This pattern is periodic and repeats itself every two pole-pairs.

Due to the decoupled nature of the electrical and magnetic circuits in MPMs the tooth number does not influence the available slot area for the coil. Tooth pitching therefore has no effect on the coil of the machine, as can be further seen in Fig. 9.

As tooth pitching has a similar effect to coil pitching in conventional machines the same classical equation for pitching factor can be used, the pitching angle, α, is set to minimise the pitching factor, k_p, for the harmonic of interest, n as follows;

$$k_p = \cos(\frac{n\alpha}{2}) \quad (3)$$

This pitching factor can then be multiplied with Equation 2 to produce an overall cogging torque equation including the effect of pitching on each harmonic.

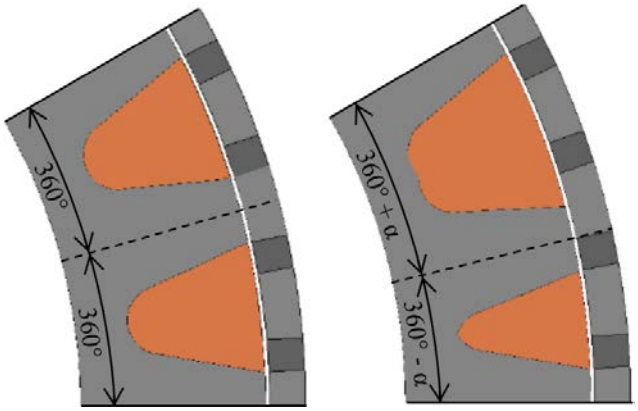

Fig. 8. Two pole-pairs of a 'fully pitched' machine (left), and two pole-pairs of a machine pitched by 60° electrical (α=60°).

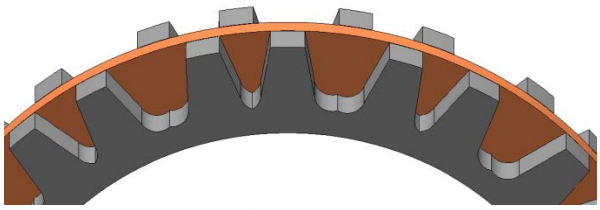

Fig. 9. Alternative view of a machine with the teeth pitched.

It has been shown above that the dominant cogging torque harmonic is the 6th. The angle, α, corresponding to a pitching factor of zero for the 6th harmonic is 30°, hence this pitching angle is used in subsequent analysis.

It is worth nothing that unlike conventional machines, where the finite number of slots result in discreet pitching angles, there are no such limitations with the position of the teeth in an MPM. Any pitching angle can be chosen regardless of the number of poles or phases, giving complete design freedom.

V. Finite Element Analysis

A. *Fully Pitched FE Model and Validation*

A fully pitched three-phase machine with the dimensions given in Table I has previously been constructed, tested, and reported by the authors [5]. Consequently measured data from a fully pitched machine has previously been compared with FEA simulations. Fig. 10 and Fig. 11 show the comparisons of measured and simulated results for both the back EMF and cogging torque.

TABLE I
Relevant Dimensions of the Prototypes.

Parameter	Value	Unit
Phases	3	
Poles	50	
Rotor Outer Diameter	159.2	mm
Airgap	0.4	mm
Stator Outer Diameter	146	mm
Axial Length	49.6	mm
Length Per Phase	15.2	mm
Stator Coreback Depth	5	mm
Phase Gap	2	mm
Magnet Dimensions (t x h x d)	3.9 x 3.5 x 49.6	mm

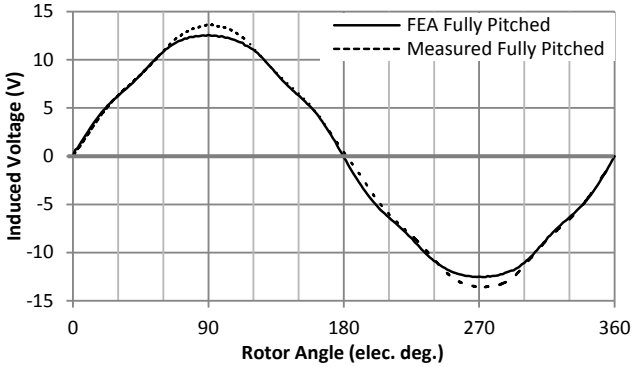

Fig. 10. Comparison of FEA and Measured EMF for the fully pitched machine, this was used to calibrate the model.

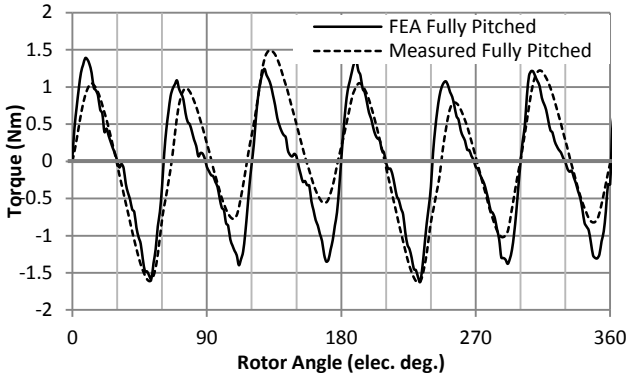

Fig. 11. Comparison of previous measured cogging torque result and FEA of the fully pitched machine, this was used to calibrate the model.

The characteristics of the waveforms are similar in both cases. The mean square error of the EMF and cogging torque are less than 5% and 10% respectively. It was therefore considered that further finite element calculations for the pitched machine could be considered valid for comparison with the fully pitched machine.

For a fair comparison between the pitched and fully pitched machines all features, except for the tooth profile resulting from pitching, were kept the same. For clarity the parameters of the machine that were identical were;

- The Dimensions - The outer diameter, inner diameter, air gap size, and active length of the machine.
- The Stator Components – Apart from the teeth of the machine the same stator components were used. The machines were built around the same shaft and hub with the same coils, meaning that to test one configuration of machine required the other to be completely disassembled and the alternative stator tooth profile assembled.
- The Rotor Components - The same rotor was used in both cases, this was modelled as being constructed from Somaloy® 3P [28] SMC rotor pole pieces and Neodymium Grade N35 magnets (B_r=1.2 T).

As a result of these constraints it is apparent that the machines will have the same space envelope, and the mass of both machines will be equal. The change in the shape of the tooth profile is in the pressing direction of the component, therefore the process is no more complicated, as a result the pitching solution will not increase the cost of the machine components.

B. *Pitched FE Model*

For the separate-phase machine without pitching it is

possible to model a single pole pair of the machine with an even periodic boundary applied to the radial edges of the simulation.

The pitched machine is only periodic in its geometry every two pole pairs, hence a larger FE model is required. This leads to a model with an increased complexity and greater computational time. The FE model of the pitched machine is shown in Fig. 12.

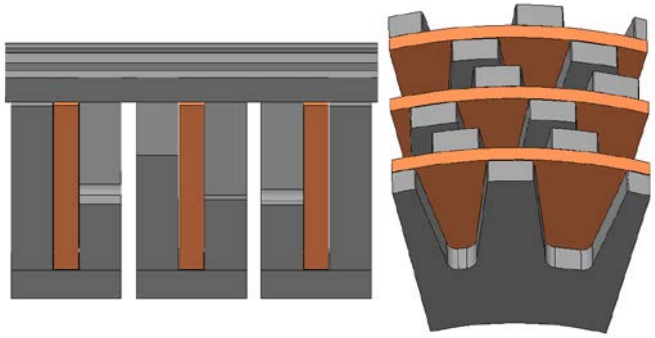

Fig. 12. Axial and projected view of the FE model for the pitched machine.

A comparison between FEA and Equation 3 has been conducted and the results are presented in Fig. 13. The fit between the classical pitching equation and the results of the FEA is shown to be very good.

The fundamental voltage is shown to decrease with pitching angle, in the same way that the fundamental voltage is reduced by pitching the coils of a conventional machine. The 5th harmonic of voltage, which is particularly high in the fully pitched machine, is reduced to near zero at a pitching angle of 36°. The 6th harmonic of cogging is lowest at a pitching angle of 30°, as is the overall cogging torque, which is now dominated by the 12th harmonic.

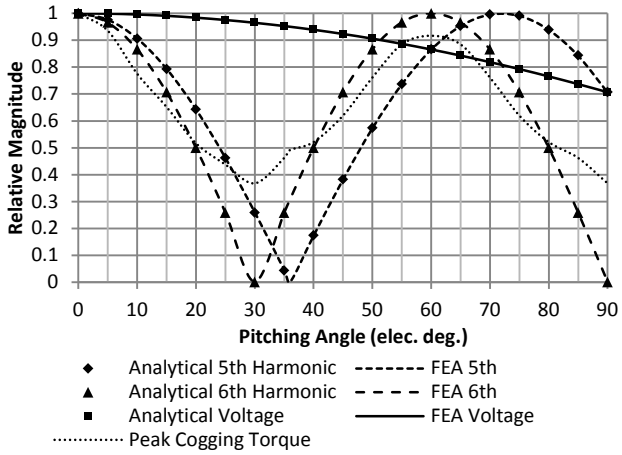

Fig. 13. Comparison of the pitching factors calculated by Equation 3 with FEA results of fundamental voltage, 5th harmonic voltage and 6th Harmonic cogging torque.

C. FE Comparison of Pitched and Fully Pitched Machine

A pitching angle of 30° electrical was applied in an attempt to eliminate the 6th harmonic of cogging torque, and reduce the 5th harmonic of voltage as was shown in Fig. 13.

Fig. 14 shows a comparison of the FEA cogging torque for both machines. The cogging torque of the pitched machine has been reduced from a peak of 1.62Nm to a peak of 0.622Nm.

The back EMF of the machine is not significantly affected by the pitching, although the EMF waveform of the pitched machine is more sinusoidal, this is due to the reduced harmonic content, and can be seen in Fig. 15. A Fourier transform was conducted on the two waveforms, the pitched machine has a slightly increased fundamental component (1.25%), this goes against Equation 3 which suggests a reduction in the back EMF of the machine as a result of pitching the teeth. This is expected to be because the reduced harmonic content picked up by the pitched teeth in their new position slightly reduces the saturation of the magnetic circuit, allowing the fundamental to increase.

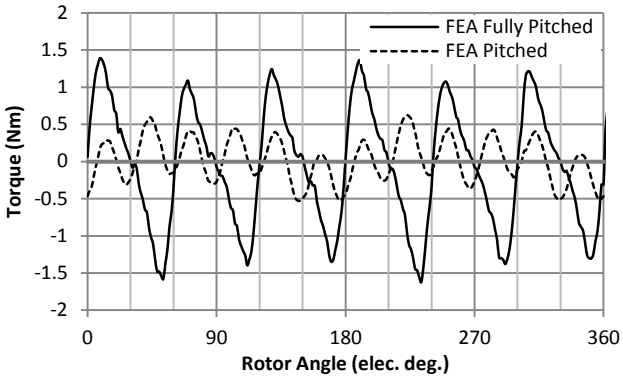

Fig. 14. Comparison of FEA cogging torque of an fully pitched and pitched machine.

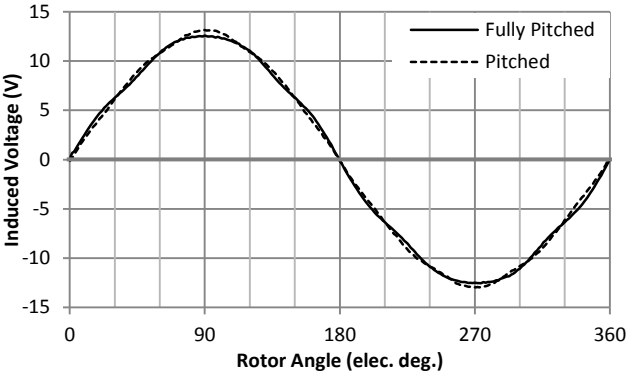

Fig. 15. Comparison of FEA back EMF for the fully pitched and pitched machines at 285rpm.

A further comparison of the static torque waveform produced by the two machines is given as Fig. 16. The static torque in this case was achieved by applying maximum current to the inner phase of the machine, with the current returning through the outer two phases in parallel. This gives a pseudo-sinusoidal operating point with 1pu,-0.5pu,-0.5pu current in the inner and outer phases respectively. The rotor was then rotated through a half electrical cycle to calculate the torque with position.

The thermally rated current for these machines is 20A, at this current the average torque of the pitched machine is 2.5% greater.

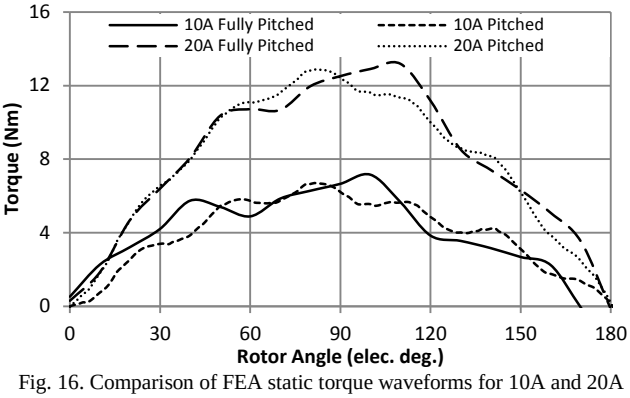

Fig. 16. Comparison of FEA static torque waveforms for 10A and 20A applied current.

VI. Experimental Results

A. Experimental Setup

A fully pitched MPM already existed from previous work. The only difference between original and pitched machines is the tooth profile, all other components were reused: the rotor, stator hub, shaft, bearings and coils, and all associated insulation.

Fig. 17 and Fig. 18 illustrate the fully pitched and pitched machines, and Fig. 19 shows a close up view of the flux concentrating rotor.

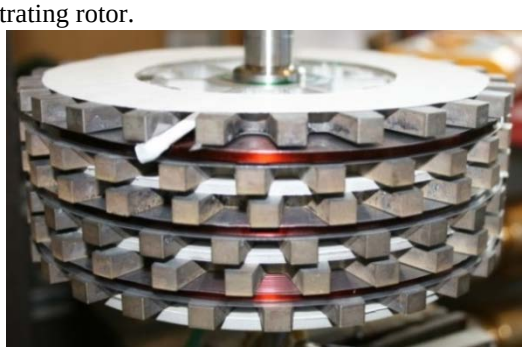

Fig. 17. Axial view of the fully pitched machine.

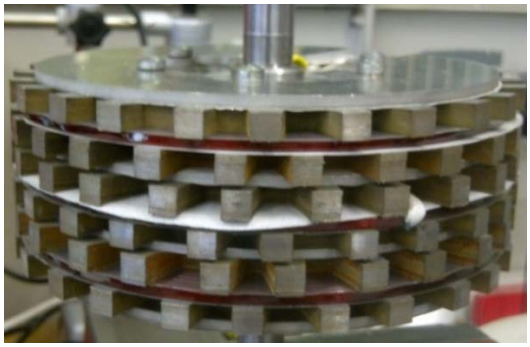

Fig. 18. Axial view of the pitched machine the teeth can be seen to be closer at some points and further away at others.

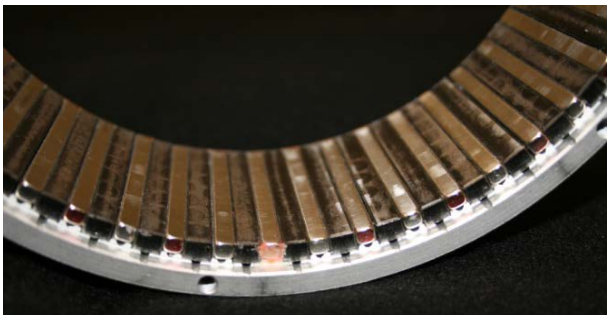

Fig. 19. Close up view of flux concentrating rotor, the NdFeB magnets are light and the SMC pole pieces are dark.

B. Cogging Torque Measurement and Comparison

Fig. 20 shows the experimental rig, consisting of a rotary dividing head to rotate and hold the machine at small angular increments (in this case $^1/_{12}{}^{th}$ of a degree). This was coupled to a 2Nm Magtrol™ torque transducer, the output of which is fed into a data acquisition unit linked to a PC.

The cogging torque of the two machines is shown in Fig. 21. The pitched machine exhibits a significantly lower peak cogging torque, which has been reduced from 1.70Nm to 0.446Nm. This is a 74% reduction, reducing the peak cogging torque to less than 3% of the machines rated torque.

The pitching aimed to suppress the 6th harmonic. It can be seen in Fig. 22 that this harmonic was significantly reduced. The 12th harmonic is now significant. It must be noted that the 12th harmonic could also be reduced by further tooth pitching. Pitching for one harmonic requires the teeth to be grouped into sets of two, where each tooth is alternately pitched clockwise or anti-clockwise. It is the case that if these groups of two are also pitched against each other for the 12th harmonic, then this can also be reduced, leading to a further reduction in cogging torque. The fundamental back EMF would be reduced further by this pitching with the total reduction being equal to the multiple of the pitching factor of the 6th and 12th harmonics.

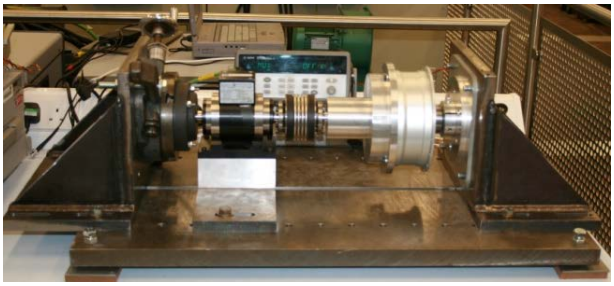

Fig. 20. The experimental test setup, consisting of a rotary dividing head, torque transducer and the machine under test.

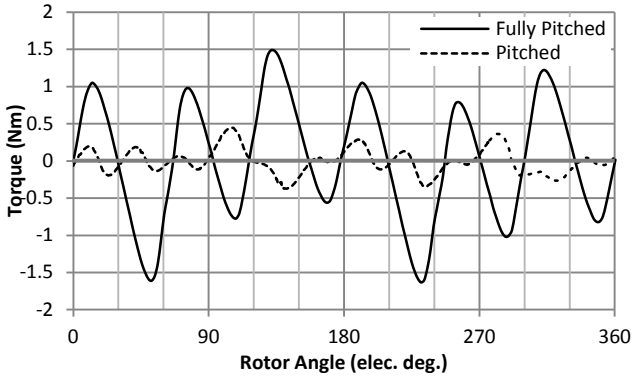

Fig. 21. Comparison of the measured cogging torque of the fully pitched and pitched machines.

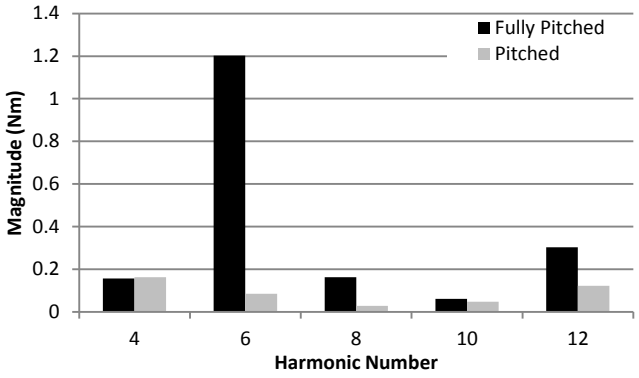

Fig. 22. Harmonic content of the cogging torque of the fully pitched and pitched machines.

C. Back EMF Measurement and Comparison

The three phase back EMFs of both machines are shown in Fig. 23 and Fig. 24 to illustrate that the pitched machine retains the balance between the phases. In both cases it can be seen that the inner phase (Phase B) has a higher magnitude than the two outer phases, this is also the case in FEA models of the machine. There are two causes;

1. The inner phase of the machine has an equal contribution of mutual inductance from both adjacent

outer phases. The outer phases however do not have this, as they are adjacent to only the inner phase. This means that mutual leakage fluxes affect the middle phase more than the outer phases.

2. As the rotor spans all three phases with no gaps, there are SMC and magnet sections above the stator phase separation gaps. The inner phase couples both of these additional rotor sections, whereas the outer phases couple only one.

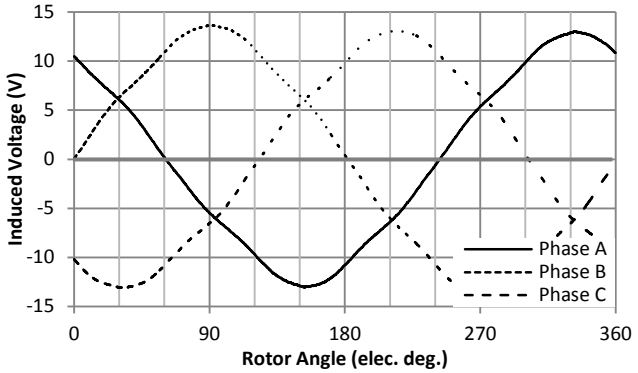

Fig. 23. The three phase back EMFs of the fully pitched machine at 285rpm.

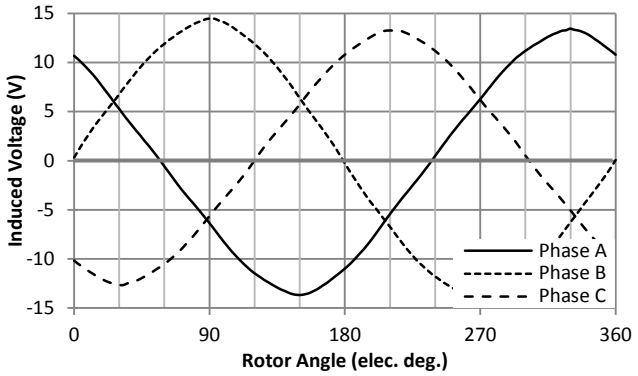

Fig. 24. Three-phase back EMFs of the pitched machine at 285rpm.

The phase back EMFs for both machines are compared in Fig. 25, along with the harmonic content in Fig. 26. The pitched machine, as in the simulations, has a slightly larger fundamental back EMF (101.8% of the fully pitched) and a reduced 5th harmonic component (36.5%), this is less than would be expected from Equation 3, which predicts a reduction to 25.9% of its original value.

As the machines are star connected the triplen harmonics are not considered important. The line to line values of back EMF have also been analysed and show that the pitched machine provides a reduction in total harmonic distortion (THD) from 3.30% to 0.64%.

D. Static Torque and Torque Ripple Comparison

The static torque of the machines was measured using the same test setup as was shown in Fig. 20, with the addition of a DC power supply to provide the required torque producing current to the windings of the machine.

As with the FEA model earlier the inner winding of the machine was connected in series with the outer two windings in parallel. This leads to maximum current being applied to the inner phase, with half the current returning through each of the outer two phases.

The rotor was rotated through a half electrical cycle in steps of $^{1}/_{12}^{th}$ of a mechanical degree giving the waveforms shown in Fig. 27.

At a current of 20A the average torque of the pitched machine is 7.67Nm, compared to 7.41Nm for the fully pitched machine. This is a small increase of 3.5%, greater than expected from FE calculations.

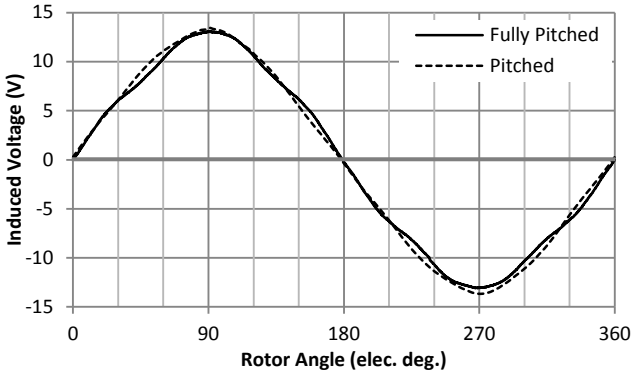

Fig. 25. Comparison of fully pitched and pitched back EMF waveforms at 285rpm.

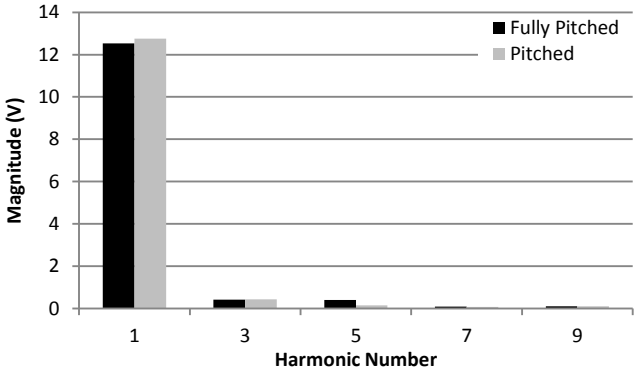

Fig. 26. Harmonic content of the phase Back EMF waveforms of both machines (the average content of all three phases).

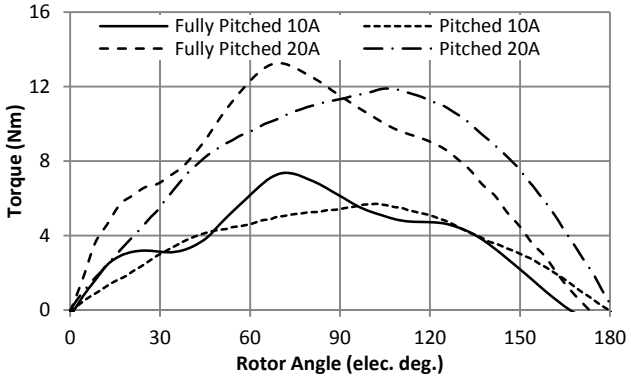

Fig. 27. Comparison of static torque waveforms for 10A and 20A applied currents.

E. Pitched FEA Model Validation

A comparison of the pitched machine with the simulated FEA data is presented in Fig. 28 and Fig. 29. This compliments the initial finite element validation of the fully pitched machine presented in Fig. 10 and Fig. 11, but also demonstrates that the FE model of a pitched machine has the same accuracy as the original fully pitched FE model. The measured and simulated back EMF waveforms are almost identical. The measured and simulated cogging torque waveforms show similar harmonic characteristics but a reduced magnitude for the measured results. Also presented in Fig. 30 is a comparison of FEA static torque with the measured waveform, which shows slightly more harmonic content as would be expected from the differences in the cogging torque, which is the main component of the ripple. The use of the FEA models to compare the fully pitched and pitched models is thus validated.

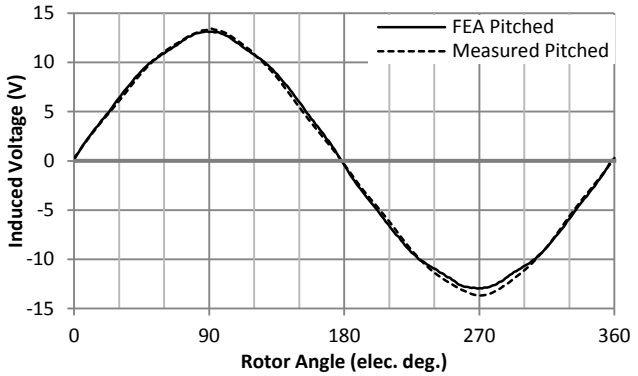

Fig. 28. Comparison of FEA and Measured EMF for the pitched machine at 285rpm.

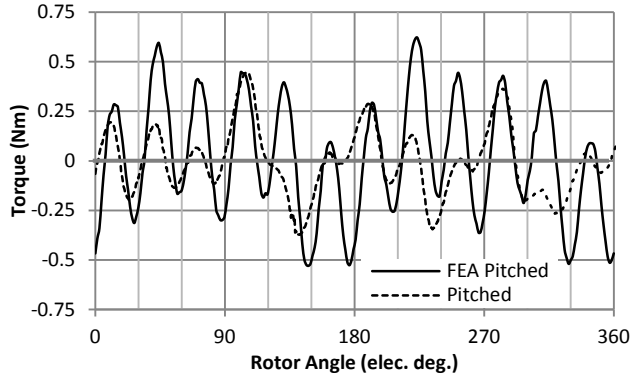

Fig. 29. Comparison of FEA and Measured cogging torque for the pitched machine.

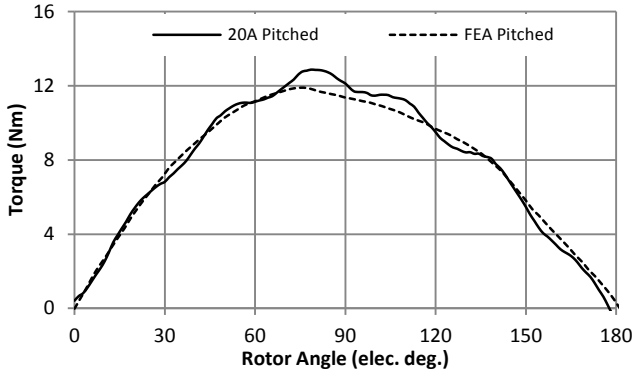

Fig. 30. Comparison of FEA and measured static torque for 20A applied current.

VII. Torque Ripple

Fig. 31 is a comparison of loaded torque for the two previously validated models. The cogging torque of the machine is by far the biggest contributor to the overall torque ripple of the machine. The pitched machine as a result of its reduction in both harmonics and cogging reduces the torque ripple at rated MMF from 17.5% to 9.3% and from 12.2% down to 7.7% at higher MMF.

VIII. Conclusion

Modulated Pole Machines are well known for their high torque densities, yet they often suffer from high cogging torque and torque ripple. This paper has analysed a method for reducing cogging torque and improving the back EMF harmonic content of MPMs.

It has been shown that the main components of cogging torque present in a three-phase MPM are the 6^{th} and 12^{th} harmonics, as all other harmonics cancel. A separate-phase MPM had already been constructed for use in a previous project, and the experimental results prove this to be the case.

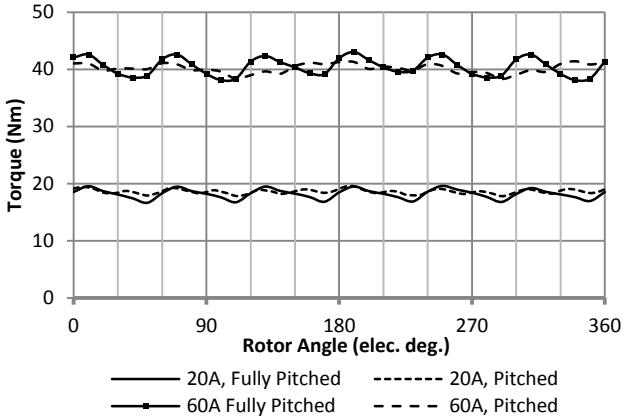

Fig. 31. FE Comparison of motor loaded torque at rated and three times rated current.

A method of tooth pitching has been used in order to cancel the 6^{th} harmonic of cogging torque, as well as to reduce the 5^{th} harmonic of back EMF. The approach is similar to coil pitching in conventional machines, where a machine is wound with the windings offset so as to reduce certain harmonic components in the back EMF. However in MPMs the coil cannot be pitched as the windings are simple hoop coils, so instead it is the teeth that have to be shifted.

In this respect MPMs have a number of benefits when pitching is used compared to conventional machines. Since moving the teeth also affects the magnetic circuit the cogging torque can be reduced along with the harmonic components of back EMF. Furthermore, because the machine is not slotted in the traditional sense the teeth can be placed at any angle around the circumference of the machine. This means that unlike the discrete slot positions of a standard machine, any harmonic number can be pitched for no matter what the pole/tooth number of the MPM.

In order to assess the validity of the concept both finite element and experimental results were obtained. A machine pitched for the 6^{th} harmonic was built, tested, and compared with the fully pitched separate-phase machine, the results are summarised in Table II.

TABLE II
Comparison of the Fully Pitched and 30° Electrical Pitched Machines

Parameter	Fully pitched	Pitched
Peak Cogging Torque	1.70Nm	0.446Nm
Peak Back EMF	13.25V	13.79V
Back EMF (Vrms)	8.87V	9.17V
Peak Fundamental Back EMF	12.52V	12.75V
THD of Line to Line Back EMF	3.30%	0.64%
Average Torque (20A Applied)	7.41Nm	7.67Nm

Overall the pitched machine produced a back EMF that was higher than that of the original fully pitched machine, whilst reducing the cogging torque by 74%, and the THD of the line to line voltages to 0.64%.

The average torque of the pitched machine measured statically over half an electrical cycle was increased by 3.5% over the fully pitched machine.

Another important factor is that the number of components in the machine is unchanged; production of the

pitched stator component is possible using the same manufacturing process as the fully pitched machine, therefore from a manufacturing point of view this cogging torque reduction method is free.

IX. References

[1] H. Weh and H. May, "Achievable force densities for permanent magnet machines in new configurations," *Proc. Int. Conf. Electrical Machines (ICEM86)*, 1986.

[2] B. C. Mecrow, A. G. Jack, and C. P. Maddison, "Permanent Magnet Machines for High Torque, Low Speed Applications," *Proc. Int. Conf. Electrical Machines (ICEM96)*, vol. 3, pp. 461-466, 1996.

[3] R. Blissenback, U. Schafer, W. Hackmann, and G. Henneberger, "Development of a transverse flux traction motor in a direct drive system," *Proc. Int. Conf. on Electrical Machines (ICEM2000), Helsinki, Finland*, vol. Volume III, pp. 1457-1460, 2000.

[4] M. Dubois, H. Polinder, and J. A. Ferreira, "Effect of air gap thickness on transverse-flux permanent magnet (TFPM) machine with flux-concentration," *Proc. Int. Conf. on Electrical Machines (ICEM2002), Brugge, Belgium*, 2002.

[5] Washington, J.G.; Atkinson, G.J.; Baker, N.J.; Jack, A.G.; Mecrow, B.C.; Jensen, B.B.; Pennander, L.; Nord, G.L.; Sjöberg, L., "Three-Phase Modulated Pole Machine Topologies Utilizing Mutual Flux Paths," *Energy Conversion, IEEE Transactions on* , vol.27, no.2, pp.507,515, June 2012.

[6] C. P. Maddison, B. C. Mecrow, and A. G. Jack, "Claw Pole Geometries for High Performance Transverse Flux Machines," *Proc. Int. Conf. on Electrical Machines (ICEM98), Istanbul, Turkey*, pp. 340-345, 1998.

[7] M. R. Dubois, N. Dehlinger, H. Polinder, and D. Massicotte, "Clawpole Transverse-Flux Machine with Hybrid Stator," *Proc. Int. Conf. on Electrical Machines (ICEM2006)*, 2006.

[8] P. Dickinson, A. Jack, and B. Mecrow, "Improved permanent magnet machines with claw pole armatures," *Proc. Int. Conf. on Electrical Machines (ICEM2002), Brugge, Belgium*, 2002.

[9] E. Schmidt , "3-D finite element analysis of the cogging torque of a transverse flux machine," *Magnetics, IEEE Transactions on*, vol. 41, pp. 1836-1839, 2005.

[10] E.Schmidt, "Finite element analysis of a novel design of a three phase transverse flux machine with an external rotor," *Magnetics, IEEE Transactions on*, vol. 47, pp. 982-985, 2011.

[11] M. Dubois. "Optimized permanent magnet generator topologies for direct drive wind turbines", Ph.D. dissertation, Delft University of Technology, Delft, The Netherlands, 2004.

[12] Polinder, H.; Mecrow, B.C.; Jack, A.G.; Dickinson, P.G.; Mueller, M.A.; , "Conventional and TFPM linear generators for direct-drive wave energy conversion," *Energy Conversion, IEEE Transactions on* , vol.20, no.2, pp. 260- 267, June 2005.

[13] G. Henneberger and M. Bork, "Development of a new transverse flux motor," in *New Topologies for Permanent Magnet Machines (Digest No: 1997/090), IEE Colloquium on*, 1997, pp. 1/1-1/6.

[14] M. R. Harris, G. H. Pajooman, and S. M. Abu Sharkh, "The problem of power factor in VRPM (transverse-flux) machines," in *Electrical Machines and Drives, 1997 Eighth International Conference on (Conf. Publ. No. 444)*, 1997, pp. 386-390.

[15] Favre, E.; Cardoletti, L.; Jufer, M., "Permanent-magnet synchronous motors: a comprehensive approach to cogging torque suppression," *Industry Applications, IEEE Transactions on* , vol.29, no.6, pp.1141,1149, Nov/Dec 1993.

[16] Masmoudi, A.; Njeh, A.; Mansouri, A.; Trabelsi, H.; Elantably, A., "Optimizing the overlap between the stator teeth of a claw pole transverse-flux permanent-magnet Machine," *Magnetics, IEEE Transactions on* , vol.40, no.3, pp.1573,1578, May 2004.

[17] Ji-Young Lee; Jung-Hwan Chang; Do-Hyun Kang; Sung-Il Kim; Jung-Pyo Hong, "Tooth Shape Optimization for Cogging Torque Reduction of Transverse Flux Rotary Motor Using Design of Experiment and Response Surface Methodology," *Magnetics, IEEE Transactions on* , vol.43, no.4, pp.1817,1820, April 2007.

[18] Heetae Ahn; Gunhee Jang; Junghwan Chang; Shiuk Chung; Dohyun Kang, "Reduction of the Torque Ripple and Magnetic Force of a Rotatory Two-Phase Transverse Flux Machine Using Herringbone Teeth," *Magnetics, IEEE Transactions on* , vol.44, no.11, pp.4066,4069, Nov. 2008.

[19] Njeh, A.; Masmoudi, A.; Elantably, A., "3D FEA based investigation of the cogging torque of a claw pole transverse flux permanent magnet machine," in *Electric Machines and Drives Conference, 2003. IEMDC'03. IEEE International* , vol.1, no., pp.319-324 vol.1, 1-4 June 2003

[20] Deodhar, R. P.: Pride, A: "Claw Pole Stator" Patent GB2491880 Filed 16/06/11 Granted 03/03/15.

[21] Deodhar, R.P.; Pride, A.; Bremner, J.J., "Design Method and Experimental Verification of a Novel Technique for Torque Ripple Reduction in Stator Claw-Pole PM Machines," in Industry Applications, IEEE Transactions on , vol.51, no.5, pp.3743-3750, Sept.-Oct. 2015.

[22] Dreher, F.; Parspour, N., "Reducing the cogging torque of PM Transverse Flux Machines by discrete skewing of a segmented stator," in Electrical Machines (ICEM), 2012 XXth International Conference on , vol., no., pp.454-457, 2-5 Sept. 2012.

[23] Hanselman, D.C.; , "Effect of skew, pole count and slot count on brushless motor radial force, cogging torque and back EMF," *Electric Power Applications, IEE Proceedings* - , vol.144, no.5, pp.325-330, Sep 1997.

[24] Zhu, Z.Q.; Ruangsinchaiwanih, S.; Schofield, N.; Howe, D.; , "Reduction of cogging torque in interior-magnet brushless machines," *Magnetics, IEEE Transactions on* , vol.39, no.5, pp. 3238- 3240, Sept. 2003.

[25] Y. G. Guo, J. G. Zhu, and H. Y. Lu, "Accurate determination of parameters of a claw-pole motor with SMC stator core by finite-element magnetic-field analysis," *Electric Power Applications, IEE Proceedings* -, vol. 153, pp. 568-574, 2006.

[26] Oudet C, 1985, "Method and Apparatus for Harmonics Suppression in Motor Systems", Patent US4629916, Granted 16/12/1986.

[27] Kastinger, G.; Schumacher, A., "Reducing torque ripple of transverse flux machines by structural designs," *Power Electronics, Machines and Drives, 2002. International Conference on (Conf. Publ. No. 487)* , vol., no., pp.320,324, 4-7 June 2002.

[28] "Somaloy technology for electric motors," (Mar. 2011). [Online]. Available: http://www.hoganas.com.

[29] Masmoudi, A.: Elantably, A. "A simple assessment of the cogging torque in a transverse flux permanent magnet machine" Electric Machines and Drives Conference, 2001, p754-759.

X. Biographies

Jamie G. Washington received his B.Eng. and Eng.D. degrees from Newcastle University, Newcastle Upon Tyne, U.K., in 2008 and 2012 respectively. His Eng.D. focused on high-torque low-speed machines constructed using soft magnetic composites.

He is currently working as a Development Engineer at Höganäs AB, Höganäs, Sweden. His main focus is the development of torque-dense traction motors utilising soft magnetic composite materials.

Glynn J. Atkinson received the M.Eng. degree in electrical and electronic engineering from Newcastle University, Newcastle Upon Tyne, U.K., in 2001. His EngD degree focused on fault-tolerant machines for aerospace applications, focusing on high-power, high-speed permanent magnet machines. He is now a Senior Lecturer within the Electrical Power Research group leading research into 3-D machine topologies using soft magnetic composites with applications in the automotive and high volume manufacturing sectors and is also researching electrical machine design for fault tolerance in aerospace applications.

Nick J. Baker received an M.Eng Degree in Mechanical Engineering from Birmingham University, UK, in 1999. He obtained a PhD in electrical machine design for marine renewable energy devices from Durham University, UK, in 2003. He has held a research post in machine design at Durham University in addition to academic posts within Lancaster University's Renewable Energy Group (2005-2008) and, presently Newcastle University's Electrical Power Group. Nick has spent a period in industry as a senior consultant for energy consultancy TNEI in Newcastle, UK (2008-2010).

He is presently working on machines across the renewable, automotive and aerospace sectors.